International Journal of Automotive Research, Vol. 9, No. 1, (2019), 2918-2933

Iran University of Science and Technology

International Journal of Automotive Engineering

Journal Homepage: ijae.iust.ac.ir

ISSN: 2008-9899

Radiation modeling of a turbulent diffusion flame in diesel engine

M.pishgooie[1], S.M.Hosseini Sarvari[2], S.H. Mansouri[3] *

[1]Phd student shahid bahonar university of kerman

[2]Proffessor of shahid bahonar university of kerman

[3] Proffessor of shahid bahonar university of kerman

ARTICLE INFO

Article history:

Received : 2018/09/20

Accepted: 2019/03/20

Published:

Keywords

Radiation

Combustion

None-gray Media

OpenFoam

Soot

A B S T R A C T

The purpose of this study is to investigate the effect of radiation heat transfer on temperature distribution and heat flux to the walls of a diesel engine. A diffusion flame is modeled in a simple cylindrical geometry and boundary conditions are defined. A specific solver which can model the turbulent diffusion flame by considering radiation in participating media is used to solve the problem. The solver is verified using experimental data of a furnace. The results show that with considering radiation and non-gray effects in the model, the flame temperature is calculated higher than that with ignoring these effects (about 11% in problem considered in this study).

1. Introduction

Internal Combustion engine studies can be of high importance due to their large applications in transportation, industry and so on. Despite the appearance of new energy technologies, the role of fossil fuels cannot be ignored in long term period, because of economic concerns. Therefore, studies in the field of internal combustion engines are very important .In this study, among all the researches in the field of internal combustion engines, simultaneous solving of combustion problem and radiation heat transfer problem is considered [1]. Radiation can play an important role in temperature distribution and heat transfer to walls of combustion chamber. Based on theories of radiative heat transfer, as temperature and participating media concentration increases in an environment, radiative heat transfer will become more important [2]. For example, in diesel engines and in particular low-speed diesel engines, ignoring radiation in the combustion chamber leads to high level of errors in heat transfer to wall and temperature distribution in combustion chamber. In addition, prediction of soot formation and nitrogen oxide production which are important subjects in internal combustion engines study, require more detailed modeling tools and experimental analysis to be conducted [3].

Combustion and radiative heat transfer are among complex problems in engineering because they depend on interrelated and complicated sub processes, like turbulence and chemical kinetics [2]. For example, turbulence and chemical reactions are coupled in highly nonlinear ways, leading to entirely new classes of interactions, namely the turbulence–chemistry interaction (TCI). Turbulence also influences transport processes in flames and heat release and in turn temperature influences turbulence by changes in the temperature-dependent properties leading to entirely new classes of interactions, turbulence–Radiation interaction (TRI) [4]

*Corresponding Author
Email Address: mansouri@alum.mit.edu
10.22068/ijae.9.1.2918

[DOI: 10.22068/ijae.9.1.2919]

The first studies of heat transfer in internal combustion engines leads to experimental relations, say Nusselt-Reynolds relation, which has different accuracy for different problems [5]. In 1967 Woschni [6] developed an experimental relation to estimate heat transfer in cylinder without considering radiation. Annand in 1971 proposed an experimental relation which consider radiation heat transfer. He used the averaged gas temperature in the cylinder for radiation calculations which may leads to error, especially in systems with significant temperature gradient. Hence, the relation is not so accurate and it is not applicable for all types of problems [7]. In 1982, Mansouri and Heywood [8] developed a model for a diesel engine with divided combustion chamber. The novel feature of their model was the use of a stochastic mixing approach during the combustion and expansion processes to describe the non-uniform fuel-air ratio distribution within the engine. To estimate the in-cylinder heat transfer, they used a Nusselt-Reynolds correlation form in which a variable length scale, based on the instantaneous cylinder height, and a variable velocity based on instantaneous mean kinetic energy in the cylinder, were used. They used a constant percentage of convective heat transfer to account for radiative heat transfer. Their model predictions agrees well with the heat released calculations based on measured data in cylinder pressures. The cycle-simulation results show that NO forms primarily in the pre-chamber. The soot studies show that soot oxidation occurs in the pre- and main-chambers, and soot oxidation mechanism is both kinetically and mixing limited. Chang et.al [9] developed a theoretical model of radiation heat transfer in diesel combustion. To compute space-resolved adiabatic flame temperature the burned fuel/air ratio distribution was inferred from the species data, for the computation of the spectral emissivity of an isothermal volume of adiabatic temperature containing soot, the Rayleigh-limit expression was used. The refraction indices in the expression were obtained by using the dispersion equations based on the electronic theory encompassing both free and bound electrons. For the spectral emissivity from the gaseous components in the volume, a semi-empirical band model was used. In 1992 Blunsdon et al. [10] modeled a multi-dimensional RTE equation for a diesel engine using KIVA code. They also developed a CFD code using discrete ordinate method (DOM) for the same problem [11]. In 2001, Mansouri et. al [12] considered engine heat transfer in order to study pollution formation in a stratified charge engine. They used a Nusselt-Renolds correlation based on rapid compression expansion machine experiments. In addition, using a zero-dimensional K-ε model, they calculated the velocities for heat transfer calculations, which has only one empirical constant for each process in the four-stroke cycle to determine the velocity for use in Reynolds number calculation (in contrast to Woschni's equation in which separate constants are used) [13]. Comparison of the model predictions with available experimental data shows a good agreement. Moreover, the program has a high flexibility for parametric studies to calculate performance parameters such as thermal efficiency, pressure, specific fuel consumption, temperature, fluid flow into and out of the cylinder, friction losses, heat transfer, and flow field in the cylinder and so on. Park [14] in 2009 developed a model for engine heat transfer considering density variation in the media in his PHD thesis. In order to increase the accuracy a density variation in the cylinder was considered and a new model, named variable density heat transfer (VDHT), was developed. Mirko [15] in 2014 studied fundamental of heat transfer in internal combustion engines modeling. He implemented a large number of simulations to evaluate the ability of different steady state CFD models in capturing impinging jet heat transfer. The work was then extended to transient CFD models. It was observed that the impinging jet-like flow occurring in a diesel engine differs from the cases available in literature in a number of important characteristics.

As mentioned above, many efforts have been made to solve the problem of combustion and heat transfer which indicates the importance of this subject. Among all modes of heat transfer, radiative heat transfer is complicated and important. However, most previous researchers used empirical formulas and constant coefficient to account for radiation. In order to investigate the effect of radiative heat transfer in an internal combustion engine, a model is used which can model combustion, turbulence, radiative heat transfer, chemical reaction etc. Then a cylindrical geometry as defined in section 3 is made to study the radiation effects on the distribution of temperature and heat transfer to the wall of an internal combustion diesel engine. The flow is assumed to be symmetric. However, in a real internal combustion engine, the flow in the cylinder is not symmetrical due to the presence of in-cylinder flows, such as swirl and squish. Since these flows affect the mixing of fuel and air and do not have effect on radiation heat transfer, assuming the simulated symmetric flow is a good assumption. The piston motion is neglected, while in a real internal combustion engine, the piston is a moving wall. This assumption can simplify the

[DOI: 10.22068/ijae.9.1.2919]

problem and due to the sudden nature and high speed of combustion process, there is not a significant change in the displacement of the piston [1].

2. Definition of the problem

To simulate the geometry of the combustion chamber of the diesel engine, a simple cylinder is used which is shown in figure 1

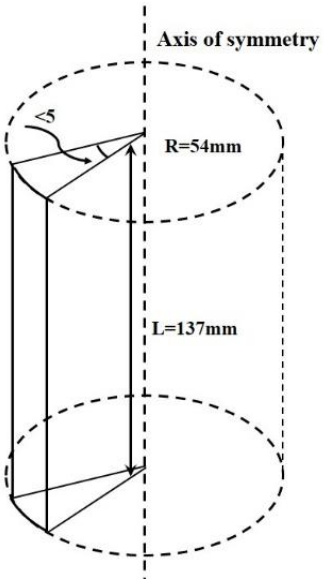

Figure 1: Geometry of the problem

Cylinder is a simple model for the internal combustion engine combustion chamber. The overall shape is similar and the differences are in details. Ignoring these details reduces the computational time and also the rate of divergence. The cylinder radius is 54 mm and its length is 137 mm, a 0.0001mm hole diameter injector is located in the center of cylinder injecting n-Heptane in 15 Mpa and 373 K into the cylinder [1].

Main assumptions in the problem are:

1. None premixed turbulent flame

2. Axisymmetric flow.

3. Ignoring moving wall.

4. Boundary and initial conditions are:

5. Inlet and exit of the cylinder is considered patch walls and axis of symmetry is considered empty.

Before fuel injection, carbon dioxide, water vapor, nitrogen and oxygen exist homogenously in the cylinder and their initial values are 0.1537 mol for carbon dioxide, 0.325 mol for water vapor, 0.7645 mol for nitrogen and 0.1092 mol for oxygen.

The initial temperature is assumed to be 1000 K

3. Modeling the problem

After defining the geometry of the problem, it is necessary to construct a solver. This solver must act in such a way that it takes into account all the considerations of the problem defined. To solve the problem, the most important properties of the solver are:

- ✓ Modeling fluid flow using basic equations in fluid mechanics (continuity, momentum conservation equation, energy conservation Equation…)[16].
- ✓ Modeling Turbulence using K-ε model.
- ✓ Modeling multi step chemical reactions
- ✓ Modeling soot formation using Fusco based soot model [17].
- ✓ Modeling conduction and convection heat transfer as suitable terms in basic equation problem.
- ✓ Modeling radiation heat transfer using DOM method with s-4.
- ✓ Modeling non-gray media using wide band model
- ✓ Absorption coefficients are based on HITRAN database

As shown in Figure 2, the model used in this study has three interrelated sub models which are fluid dynamic model, combustion model and radiation model. Fluid dynamic model contains mass, momentum and energy conservation equations and also RANS. Radiation model whose effect is considered in energy equation contains discrete ordinate method (DOM) for solving radiative transfer equation and wide band model for solving non- gray media. Combustion model whose effect is considered in energy and mass equation uses partially stirred reactor method.

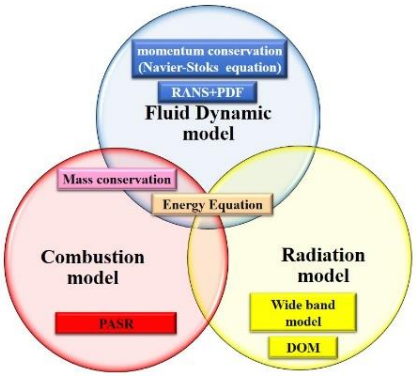

Figure 2 Model diagram

3.1. Fluid dynamic model

3.1.1. Turbulence modeling

[DOI: 10.22068/ijae.9.1.2919]

Two methods are recommended for modeling turbulence; Reynolds averaged Navier-Stoks (RANS), and large-eddy simulation (LES). In RANS, all fluctuations about the mean are modeled. In LES, the governing equations are spatially filtered, the large-scale dynamics are captured explicitly, while the effects of unresolved (sub filter) scales are modeled. LES is expected to be more accurate as compared to RANS. LES is also expected to capture phenomena that are difficult to accommodate in Reynolds-averaged approaches, such as large-scale unsteadiness. In addition, LES is three-dimensional and time-dependent, while RANS is statistically homogeneous and/or stationary to reduce the number of independent variables [4].

In order to provide a framework for describing and modeling the influences of fluctuations with respect to local mean values in RANS, or of sub filter-scale fluctuations with respect to local spatially filtered values in LES, probability density function (PDF) methods is recommended in references. In the PDF approach, the probabilities that the fluctuations in quantities of interest have particular values is considered, which are quantified by introducing a PDF, and a modeled transport equation is solved for the PDF of interest [4].

As LES is computationally intensive compared to RANS and is more likely to diverge, RANS is still of interest for practical applications. In addition, mixing RANS and PDF can solve the problems of ignoring fluctuations in RANS method. Therefore, in this study RANS model with PDF concept is used. In a turbulent flame or combustion device, estimation of the local mean value of physical quantity is of interest and can be obtained by long-time averaging in a statistically stationary flow.

Balance equations for the mean quantities in RANS

$$\frac{\partial \bar{\rho}}{\partial t} + \frac{\partial}{\partial x_i}(\bar{\rho}\tilde{u}_i) = 0 \quad (1)$$

$$\frac{\partial \bar{\rho}\tilde{u}_i}{\partial t} + \frac{\partial}{\partial x_j}\left(\bar{\rho}\tilde{u}_i\tilde{u}_j\right) = -\frac{\partial P}{\partial x_i} + \frac{\partial}{\partial x_j}\left(2(\bar{\mu} + \bar{\mu_t})\left[\tilde{S}_{ij} - \frac{1}{3}\delta_{ij}\tilde{S}_{kk}\right]\right), \tilde{S}_{ij} = \frac{1}{2}\left(\frac{\partial \tilde{u}_i}{\partial x_j} + \frac{\partial \tilde{u}_j}{\partial x_i}\right) \quad (2)$$

$$\frac{\partial}{\partial t}(\bar{\rho}\tilde{Y_k}) + \frac{\partial}{\partial x_j}(\bar{\rho}\tilde{u}_j\tilde{Y_k}) = \frac{\partial}{\partial x_j}\left(\left(\frac{\mu}{sc_k} + \frac{\mu_t}{sc_t}\right)\frac{\partial \tilde{Y_k}}{\partial x_j}\right) + \overline{\dot{\omega}_k} \quad (3)$$

k=1, 2…N

$$\frac{\partial}{\partial t}(\bar{\rho}\tilde{h}) + \frac{\partial}{\partial x_j}(\bar{\rho}\tilde{u}_j\tilde{h}) = \frac{\overline{DP}}{Dt} + \frac{\partial}{\partial x_j}\left(\left(\frac{\mu}{pr} + \frac{\mu_t}{pr_t}\right)\frac{\partial \tilde{h}}{\partial x_j}\right) - \dot{\omega}_T + S_{rad}\ ,\ \bar{\rho}\bar{\alpha} = \frac{\bar{\mu}}{pr}\ \ ,\ \ \bar{\rho}\bar{\alpha}_t = \frac{\bar{\mu}_t}{pr_t} \quad (4)$$

In Eq. (4), h is the enthalpy consists of both sensible enthalpy and enthalpy of formation [18].

3.2. Combustion model

In order to simulate combustion, partially stirred reactor (PASR) model, as general model for combustion, is used.

3.2.1. PASR Model

PASR model accounts for mixing and is computationally efficient for large coupled chemical reaction mechanisms involving many chemical species. The PASR model is described by the following partial differential equation (eq. 5), giving the evolution of the joint Composition MDF:

$$\frac{\partial F(\psi,t)}{\partial t} + \sum_{i=1}^{R+1}\frac{\partial}{\partial \psi_l}[A_l(\psi) + S_l(\psi)]F(\psi,t) = \frac{1}{\tau}\left(F_{in}(\psi) - F(\psi,t)\right) \quad (5)$$

With the initial conditions,

$$F(\psi,0) = F_0(\psi) \quad (6)$$

The MDF is represented by F, and the variable ψ represents scalars such as mass fraction of chemical species, temperature, density, etc. The right-hand side of 4 describes the inflow and outflow events in a partially stirred reactor (PaSR), with the characteristic residence time τ. S_l denotes the chemical source term for species. [19]

In the PaSR approach, a computational cell is split into two different zones: in one zone all reactions occur, while in the other one there are no reactions. Schematic of the model is presented in Fig. 5. [18]

In the PASR model, a computational cell is split up into two different zones: in one zone all reactions occur, while in the other one, there are no reaction. Schematic of the model is represented in Fig. 3 [18].

[DOI: 10.22068/ijae.9.1.2919]

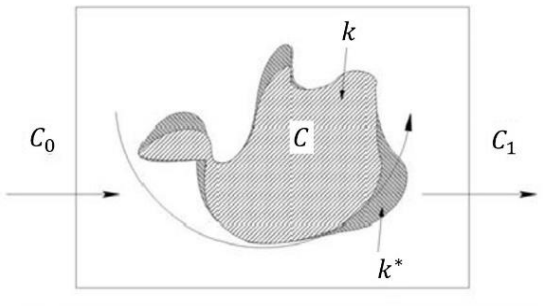

Figure 3: PASR model

Composition changes due to mass exchange with the reacting zone. In addition, the reaction zone is treated as a perfectly stirred reactor (PSR), in which all reactants are assumed to be perfectly mixed with each other. This allows neglecting any fluctuations when calculating the chemical source terms. Three average concentrations are presented in the reactor, the mean mixture concentration of the feedc_0, the mixture concentration in the reaction zone c, the mixture concentration at the exit of the reactorc_1. [18]

The whole combustion process is regarded as two processes. In the first process initial concentration in the reaction zone changes from $c_0$to c; in the second process the reacted mixture (with concentration c) is mixed with the un-reacted mixture (with concentration c_0 by turbulence), the results is the averaged concentration c1. The reaction rate of this computational cell is determined by the fraction of the reactor in this cell. It seems quite clear that it should be proportional to the ratio of the chemical reaction time τ_c to the total conversion time in the reactor, i.e. the sum of the micro-mixing time τ_{mix} and reaction timeτ_c: [18]

$$k_k = \frac{\tau_c}{\tau_c+\tau_{mix}} \qquad (7)$$

The micro-mixing time characterizes the exchange process between reactant mixture and unburnt mixture. In this study the micro-mixing time $\tau_{mix}$was obtained from the k-ε equation, the reaction time $\tau_t$was derived from the laminar reaction rate. [18]

$$\tau_{mix} = C_{mix}\sqrt{\frac{\mu+\mu t}{\rho\varepsilon}} \qquad (8)$$

3.3. Soot model

In the present work, a Fusco based soot model was implemented in the Open FOAM CFD software [16]. The base for soot calculation is a model proposed by Fusco et al. [20]. It is a phenomenological soot creation model that incorporates, via global rate expressions, the physical processes of pyrolysis, particle inception, surface growth, particle coagulation oxidation, as well as global reaction steps for intermediate species formation and oxidation for n-Heptane.

3.4. Radiation model

For an absorbing, emitting and scattering medium at position $\vec{r}$ and direction$\vec{s}$, the radiative transfer equation (RTE) is given in as:

$$\frac{dI(\vec{r},\vec{s})}{ds} = -k_\eta I_\eta(\vec{r},\vec{s}) + k_\eta I_{b\eta}(\vec{r},\vec{s}) \qquad (9)$$

where I_η and Ib,η denote the local and blackbody spectral intensity, respectively. k_η denotes the spectral absorption coefficient of participating species. This equation describes the rate of change of radiation intensity at position $\vec{r}$ along the path ds and in the direction $\vec{s}$. The RTE is solved using the discrete ordinate method (DOM).

3.4.1. Discrete ordinate method

In the discrete ordinates method, equation (10) is solved for a set of n different directions $\widehat{s_i}$ i=1,2,..., n, and the integrals over direction are replaced by numerical quadrature's, that is [21]:

$$\int_{4\pi} f(\hat{s}) = \sum_{i=1}^{n} \omega_i f(\widehat{s_i})\ G \qquad (10)$$

Once the intensities have been determined the desired direction-integrated quantities are readily calculated. The radiative heat flux, inside the medium or at a surface, may be found from its definition, equation:[22]

$$q(r) = \int_{4\pi} I(r,\hat{s})\hat{s}d\Omega \simeq \sum_{i=1}^{n} \omega_i I_i(\boldsymbol{r})\widehat{s_i} \quad (11)$$

The incident radiation G [the divergence of the radiative heat flux] is similarly determined as: [22]

$$G(r) = \int_{4\pi} I(r,\hat{s})d\Omega \simeq \sum_{i=1}^{n} \omega_i I_i(\boldsymbol{r}) \qquad (12)$$

3.4.2. Wide band Model

Band models present solutions for spectrally integrated intensities, incident radiation, and radiative heat fluxes for an absorbing-emitting medium. One of their most notable applications is radiative heat transfer formulation within combustion chambers, where the medium consists of combustion gases and soot [21]. Although exact numerical calculation of band radiation can be done using line-by-line or narrow-band models, but this model requires excessive computational times so using less detailed and computationally more efficient wide-band models which requires less

[DOI: 10.22068/ijae.9.1.2919]

computational time have been recommended in references [2].

The absorption coefficient (In this study, CO2, H2O and soot), as an input, are required as an input for DOM method. The absorption coefficients for CO2, H2O are calculated using the spectral Wide Band Box model [22]. The box model proposed by Penner [23] is the simplest wide band model. It approximates a given band with a rectangular box. The width of the band is calculated as 'effective band width', Δωe and the height of the band is determined by a mean absorption coefficient k. For a given band, 'i', the mean absorption coefficient is assumed to be constant in the given band and is related to band intensity by [22]

$$\bar{k}_\iota = \frac{S_i}{\Delta\omega_{e_i}} \quad (13)$$

The band intensity can be calculated as: [22]

$$S_i = \int_{band} k_\eta d\eta \quad (14)$$

For a gas mixture of H2O and CO2, the absorption coefficient of the mixture is obtained by simply adding the absorption coefficients of the individual species. [22]

$$\bar{k}_{\eta,g_i} = \bar{k}_{\eta,H_2o_i} p_{H_2o} + \bar{k}_{\eta,Co_{2_i}} p_{Co_{2_i}} \quad (15)$$

Where p represents the partial pressure of each specie. The radiation model access the concentration of each participating species directly from the reacting flow solver. In addition to this, the band overlap error is also taken into consideration in the current Wide Band Box model. Modest [24] as well as Liu and Zhang [25] used exponential Wide Band model and first law of quantum mechanics, respectively to calculate the band mean absorption coefficients for a given species in their simulations. The polynomial relations in this study based on Haidar et.al work are developed by calculating the absorption coefficients of H2O and CO2 from latest edition of spectral radiation database HITRAN2012. [22]

For each gaseous specie and a given band, the calculations are carried out for mole fraction of 1.0 and at temperatures of 300 K, 600 K, 1000 K, 1500 K, 2000 K and 2500 K. A polynomial data fitting is then conducted. [22]

Polynomial coefficients for both H2O and CO2 can be found in Table 1.

$$\bar{k}_{\eta,g_i} = c_0 + c_1 T + c_2 T^2 + c_3 T^3 + c_4 T^4 \quad (16)$$

Band, μm						
	2.43-2.64	2.64-3	4.13-4.53	4.54-8.33	12.5-18.18	18.34-25
Co_2						
C_0		22.23	1705.68		134.86	
C_1		-3.22×10^{-2}	-2.56		-0.2	
C_2		1.79×10^{-5}	1.42×10^{-3}		1.11×10^{-4}	
C_3		-3.36×10^{-9}	-2.64×10^{-7}		-2.04×10^{-8}	
C_4						
H_2O						
C_0	32.52	30.73		40.32		-55.75
C_1	-4.99×10^{-2}	-3.98×10^{-2}		-6.00×10^{-2}		0.27
C_2	2.78×10^{-5}	2.04×10^{-5}		3.32×10^{-5}		-2.30×10^{-4}
C_3	-5.14×10^{-9}	-3.65×10^{-9}		-6.17×10^{-9}		7.46×10^{-8}
C_4						-8.54×10^{-12}

Table 1. Absorption coefficients for the Wide Band Box Model

Soot has a continuous spectrum and the radiative properties of soot depend on its concentration and distribution in the flame [26]. By considering that soot particle sizes are generally very small, these particles are assumed to be non-scattering and the soot absorption coefficient is taken in the Rayleigh scattering limit. In this study the soot absorption coefficient is calculated as [27].

$$k_{\eta,soot} = 2370 f_v T \quad (17)$$

Here, fv and T denote the soot volume fraction and local temperature, respectively. The total spectral absorption coefficient for the gas-soot mixture is then calculated as [28]

$$\bar{k}_{\eta,g_i} = \bar{k}_{\eta,H_2o_i} p_{H_2o} + \bar{k}_{\eta,Co_{2_i}} p_{Co_{2_i}} - \bar{k}_{\eta,g_i} k_{\eta,soot} \quad (18)$$

3.4.2. Effect of pressure

In an internal combustion engine, combustion chamber pressure is higher than atmosphere. Chemical reaction rate is proportional to mixture pressure. An elementary chemical reaction mechanism in which NS species are involved, is written as a set of L reversible reactions as [4]

$$\sum_{\alpha=1}^{N_s} \vartheta'_{l\alpha} M_\alpha \rightleftharpoons \sum_{\alpha=1}^{N_s} \vartheta''_{l\alpha} M_\alpha \quad (19)$$

In Eq. (19), M_α is chemical species symbol, and $\vartheta'_{l\alpha}$ and $\vartheta''_{l\alpha}$ are stoichiometric coefficients.

[DOI: 10.22068/ijae.9.1.2919]

$$\omega_{\alpha}^{\cdot} = \sum_{i=1}^{L} \left\{ \left(\vartheta_{l\alpha}^{''} - \vartheta_{l\alpha}^{'} \right) \left[k_{l,f}(T) \prod_{\beta=1}^{N_s} c_{\beta}^{\vartheta_{l\alpha}^{'}} - k_{l,r}(T) \prod_{\beta=1}^{N_s} c_{\beta}^{\vartheta_{l\alpha}^{''}} \right] \right\} \quad (20)$$

In Eq. (20) $k_{l,f}(T)$ and $k_{l,r}(T)$ are forward and reverse rate of reaction for lth reaction receptively, and cβ is molar concentration of species β.

Most reactions in combustion study are up to three-body reactions so that reaction rates can increase in proportion to up to the third power of the pressure [29]. First-order and second-order reaction kinetics also are used in most models for soot formation and oxidation. Across a wide range of combustion systems, it has been observed that the total amount of soot present scales approximately as pn, where the value of n lies between 1.0 and 2.0 for pressures ranging from 1 to _10 bar, and n falls to zero (soot saturation) at higher pressures (above 40–50 bar) [24].

As participating species concentration increases in the combustion chamber, radiative emission and absorption rates for a participating molecular gas increase, so increasing pressure for a given species will lead to change in rate of absorption and emission of participating media, and the spectral properties also vary with pressure. In combustion applications, spectral line broadening is governed by molecular collisions and is thus proportional to total pressure p. This leads to wider, more overlapping lines, making the gas "grayer" [4]. An example is given in Fig. 4, showing a small part of the spectrum for a mixture containing 1% CO2–2% H2O at varying total pressures. The areas under the curves are proportional to pressure [30].

For higher pressure, maxima decrease and minima increase due to line broadening. Still, even at 50 bar, the absorption coefficient varies by a factor of 5 across this small part of the spectrum, leaving the gas strongly non gray, although line-by-line calculations may now require less spectral RTE solutions. [30]

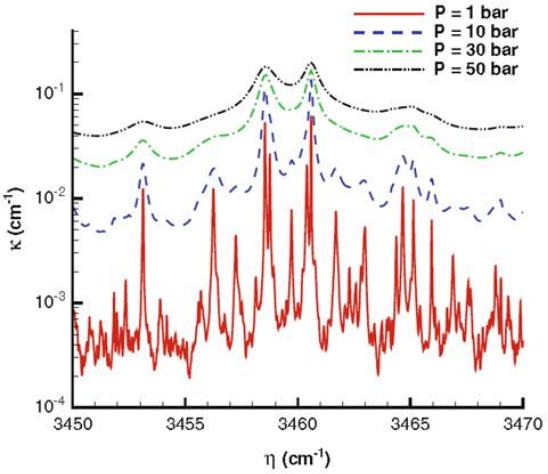

Figure. 4: Spectral absorption coefficient – wave number diagram [5]

4. Solution method

The global reaction for n-Heptane oxidation is shown in Eq. (21).

$$C_7H_{16} + 11O_2 \rightarrow 7CO_2 + 8H_2O \quad (21)$$

What actually occurs in the combustion chamber is not exactly as the global reaction, but occurrence of several sub reactions simultaneously leads to formation of final products of global reaction. In this study, for the modeling of the global reaction, about 100 sub reaction like eq.22 are considered

$$C_7H_{16} \rightarrow CH_3 + C_3H_6 + C_3H_7 \quad (22)$$

Arrhenius equation, Eq. (23), is used to calculate reaction rate:

$$k_f = AT^b . \exp(\frac{-E_a}{RT}) \quad (23)$$

Where k_f is forward reaction rate, A is pre exponential, b is the temperature exponent, Ea is the activation energy, R is the ideal gas coefficient and T is the temperature.

$$\dot{\omega_k} = \frac{d[product]}{dt} = -k_f[fuel]^n[oxidizer]^m \quad (24)$$

Where $\dot{\omega_k}$ is the chemical reaction rate, t is time, c is forward reaction order and [C] is concentration of specie C. As noted before the combustion model for this study is partially stirred reactor concept model described by Eq. (25)

$$CST_k = \frac{\tau_{chem}}{\tau_{mix}+\tau_{chem}} \dot{\omega_k} \quad (25)$$

[DOI: 10.22068/ijae.9.1.2919]

Where CSTi is the chemical source term, τ_{chem} chemical time $\propto \frac{1}{k_f}$ and τ_{mix} mixing time, which is calculated by:

$$\tau_{mix} = C_{mix}\sqrt{\frac{\mu_{eff}}{\rho\varepsilon}} \quad (26)$$

Where Cmix is a constant, μ_{eff} is the effective viscosity, ρ density and ε rate of dissipation of turbulent kinetic energy.

The chemical source term is used to calculate the local concentration of species and also thermodynamic properties using additional equations 27-29.

$$\frac{C_p}{R} = a_1 + a_2.T + a_3.T^2 + a_4.T^3 + a_5.T^4 \quad (27)$$

$$\frac{H}{RT} = a_1 + \frac{a_2.T}{2} + \frac{a_3.T^2}{3} + \frac{a_4.T^3}{4} + \frac{a_5.T^4}{5} + \frac{a_6}{T} \quad (28)$$

$$\frac{S}{R} = a_1 LnT + a_2.T + \frac{a_3.T^2}{2} + \frac{a_4.T^3}{3} + \frac{a_5.T^4}{4} + a_7 \quad (29)$$

The specific heat Cp, enthalpy H and entropy S are then used in the code to solve the conservation equations.

Knowing the local concentration of each species at any moment as their temperature, the heat transfer equations is solved assuming gray media. Radiation is solved using the discrete ordinate method and solving the non-gray environment using wide band model

The solver uses PIMPLE algorithm as shown in Figure5:

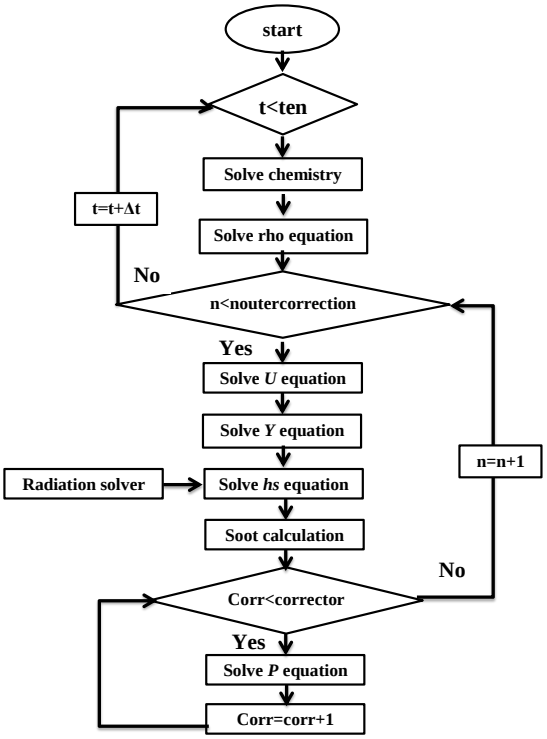

Figure 5: model flow chart

5. Model verification

Verification of the model is compared by the experimental data of a burner, namely McKenna burner, and the result are presented in figure 6

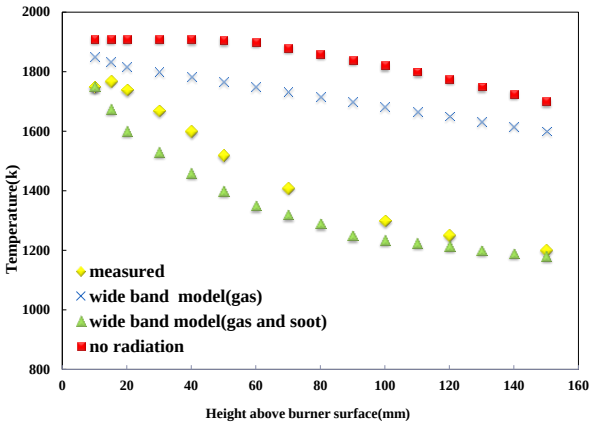

Figure6: Temperature variation along axis of symmetry of McKenna burner

For each case, the simulations are carried out first without including any radiation modeling. Then the radiation modeling is included by using constant values of absorption-emission coefficients and wide band model. The results are shown in Fig. 6 for the case of stoichiometric flame. The results show that, in absence of radiation model, the simulation predicts higher temperatures in the flame core and other measuring positions above the burner. Radiation model using gray media

[DOI: 10.22068/ijae.9.1.2919]

assumption gives good prediction of the flame temperature. However, as the heights above the burner surface increases, higher temperature values compared to the measurements are calculated by the model. The wide band model gives a lower flame core temperature but gives reasonable results at regions 90 mm and above [3]. The flame temperature profile is also predicted reasonably well. This indicates that using an improved absorption-emission model can give promising simulation results [3]. Average error in no radiation condition is about 24%, considering radiation ignoring soot formation decreases error to 17% and finally considering both radiation and soot formation results 2% average error.

6. Results and discussions

Simulation is carried out for different cases and results are presented below.

Figure 7 shows temperature distribution within the cylinder

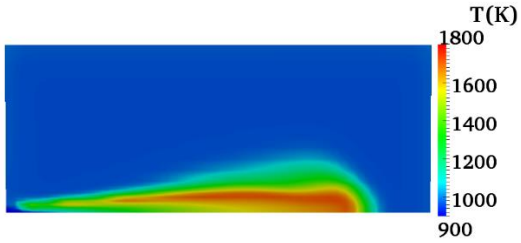

Figure 7. Temperature distribution in the cylinder

6.1. Radiation and participating media effect

Effect of radiation has been shown in Fig. 8. The figure shows Temperature variation in the center of the cylinder along the axis of symmetry in three cases; case one ignoring radiation (no radiation), in second case radiation effect is considered assuming a gray medium, and finally in third case radiation effect is considered assuming a non-gray medium.

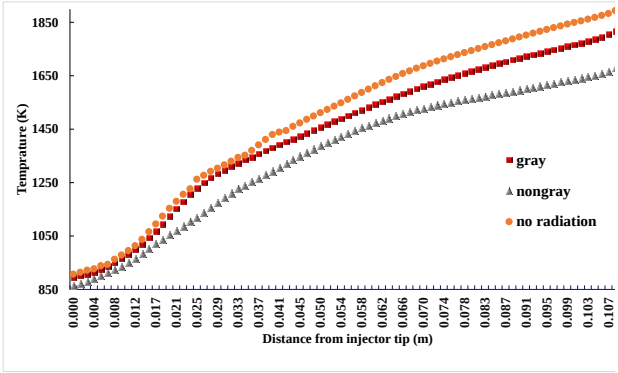

Figure 8: Temperature variation along axis of symmetry

As shown in figure 8, temperature increases along axis of symmetry. Considering radiation, the temperature is calculated less than that for no-radiation case. In addition, considering non-gray media effect will decrease the calculated temperature. In distances near injector tip, the difference between the no radiation and non-gray cases is less than 4 percent and difference between the no radiation and gray cases is less than 2 percent. Increasing the distance and temperature makes radiation effects more acute and the difference will become more than 11 percent in non-gray case and more than 4 percent in gray case. The average temperature difference with no radiation case is 3.28% in gray and 9% in non-gray case. Moreover, there is a difference between calculated temperature in gray and none gray cases. This difference differs between 2.52% to 9% and the average temperature difference is 5.92%.

Figure 9 shows temperature variation along the radial axis of in three cases; case one ignoring radiation (no radiation), in second case radiation effect is considered assuming media to be gray, and finally in third case radiation effect is considered assuming media to be non-gray.

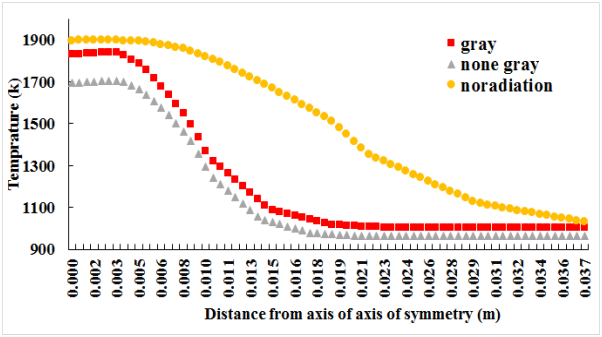

Figure 9: Radial Temperature variation

As shown in Fig. 9, as the distance from axis of symmetry increases radially, the temperature decreases. Considering radiation, the temperature is calculated less than that for no-radiation condition. In addition, considering none gray conditions, the temperature is calculated less than that for no-radiation and gray media cases. In distances far from axis of symmetry the difference between the two cases is less than 3 percent in gray and less than 7 percent considering non-gray case. In distances near the axis, increasing temperature makes radiation effects more acute and the difference will became more than 34 percent in gray and more than 38 percent considering non-gray case. The average temperature difference with no radiation condition is 17.33% in gray and 21.67% in non-gray condition. Moreover, there is a difference between calculated temperature in gray and non-gray cases. This difference differs

[DOI: 10.22068/ijae.9.1.2919]

between 2.52% to 9% the average temperature difference is 5.92%.

The results show complete compatibility with the theory. Radiation will become more important as the temperature increases, considering radiation, the temperature is calculated less than ignoring radiation, considering non-gray media effect will decrease calculated temperature. In places where the concentration of participating media increases, considering radiation and non-gray media effects will be more important.

The other important case to study here is effect of considering none gray media effect on heat transfer to cylinder wall, Fig. 10 shows local radiative heat transfer to wall in gray and non-gray cases.

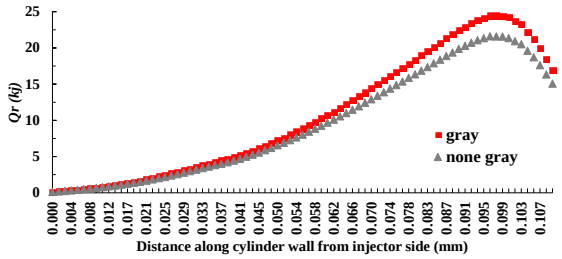

Figure 10: Radiative heat transfer to wall

As shown in Fig. 10, heat transfer to wall is a function of temperature and participating media concentration. Results show that considering gray media effect can change the result 6.23% to 11.86% and the average difference between gray and non-gray radiative heat transfer is 10.07%.

6.2. Effect of soot formation

The next important case in this study is to know the effect of soot formation in temperature gradient of combustion chamber. Soot is a participating media and Fig. 11 shows soot density distribution in the cylinder.

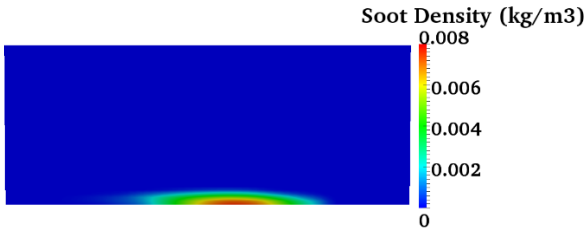

Figure 11: Soot density distribution

Figure 12 shows Temperature variation along axis of symmetry in 4 cases. In case 1, maximum density of soot in the combustion chamber is 0.0076 kg/m and the amount of maximum mass of soot is increased case by case to 0.313 gram. All other conditions are the same in all cases, but the amount of soot is different.

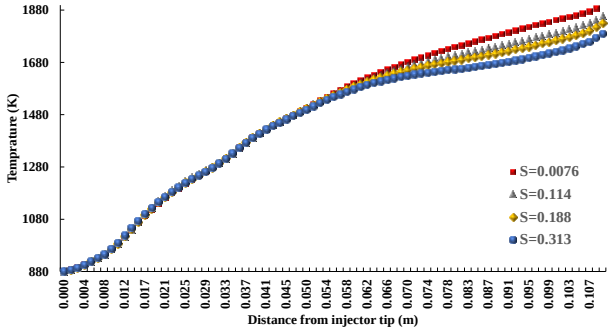

Figure 12: Soot effect on temperature variation along axis of symmetry

The results show that increasing the temperature accompanied with increasing soot formation affects temperature variation. Maximum difference between cases is about 7 percent which occurs in maximum temperature, note that this difference is obtained when soot concentration become about 42 times more.

Figure 13 shows the temperature variation in radial axis for 4 cases. The results show that increasing the temperature accompanied with increasing soot formation affects temperature variation. Maximum difference between cases is about 6 percent which occurs in maximum temperature

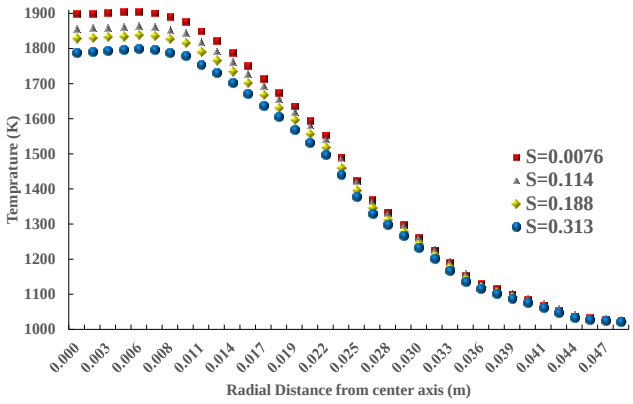

Figure 13: Soot effect on Radial Temperature variation

Figure 14 shows heat transfer to walls in different soot concentration.

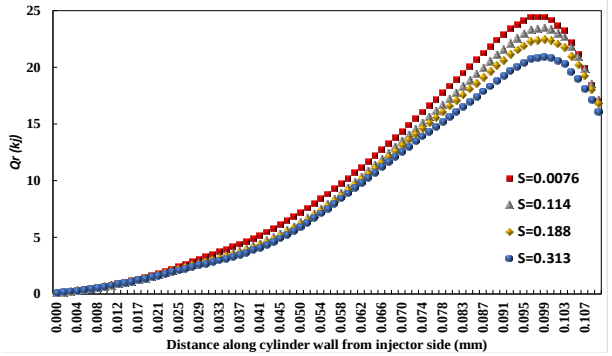

[DOI: 10.22068/ijae.9.1.2919]

Figure 14: Soot effect on heat transfer to walls

Results shows that increment of soot will decrease the amount of heat received by cylinder wall. Maximum difference is calculated about 22% in case 4.

6.3. Effect of carbon Dioxide formation

The next step in this study is to know the effect of Carbone Dioxide formation in temperature gradient of combustion chamber. Figure 15 shows carbon dioxide distribution in the cylinder.

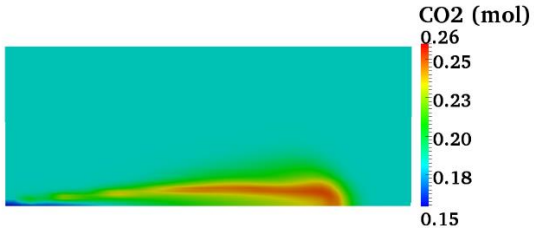

Figure 15: Carbone Dioxide distribution in the cylinder

Figure 16 shows Temperature variation along axis of symmetry for 4 cases. In case 1 maximum concentration of carbon dioxide in the combustion chamber is 0.17mol and the amount of maximum of carbon dioxide is increased case by case to 0.24mol. All other conditions are the same in all cases, but amount of carbon dioxide is different.

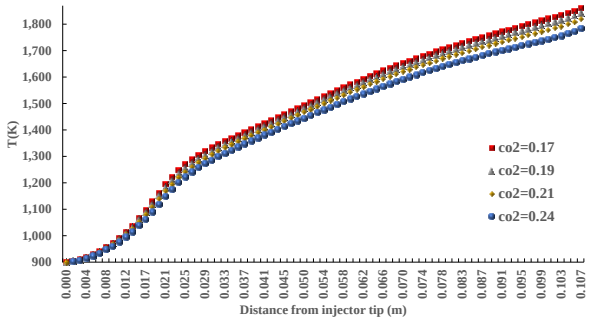

Figure 16: Carbone Dioxide effect on temperature variation along axis of symmetry

The results show that increasing the temperature accompanied with increasing carbon dioxide formation affects temperature variation. Maximum difference between cases is about 4.3 percent which occurs in maximum temperature, note that this difference is obtained when carbon monoxide concentration will become about 41% more.

Figure 17 shows Temperature variation in radial axis for 4 cases. The results show that increasing the temperature accompanied with increasing carbon dioxide formation affects temperature variation. Maximum difference between cases is about 4.27 percent which occurs in maximum temperature.

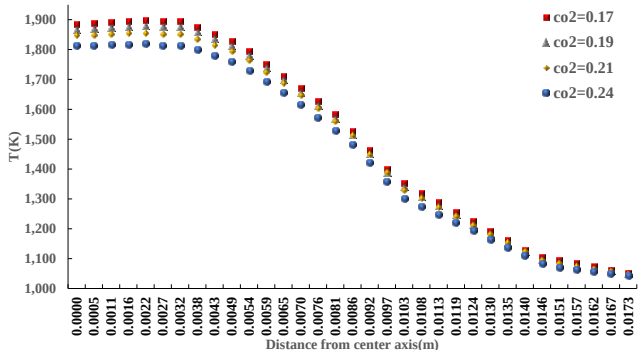

Figure 17: Carbone Dioxide effect on radial temperature distribution

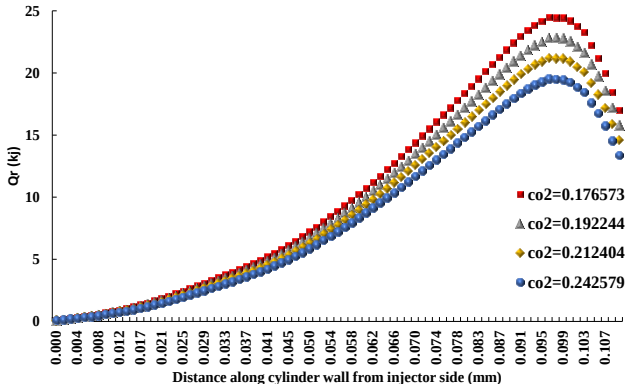

Figure 18: Carbone dioxide effect on heat transfer to walls

Figure 18 shows heat transfer to walls in different Carbone Dioxide concentration. Results show that increment of carbon dioxide will decrease the amount of heat received by cylinder wall. Maximum difference is calculated about 21% in case 4.

6.3. Effect of water vapor formation

The next step in this study is to know the effect water vapor formation in temperature gradient of combustion chamber. Figure 19 shows water vapor distribution in the cylinder.

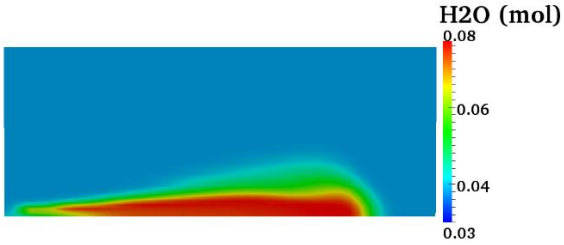

Figure 19: Water vapor distribution in the cylinder

Figure 20 shows Temperature variation along axis of symmetry for 4 cases. In case 1, maximum concentration of water vapor in the combustion chamber is 0.067mol and the amount of maximum

[DOI: 10.22068/ijae.9.1.2919]

of water vapor is increased case by case to 0.165mol. All other conditions are the same in all cases, but the amount of water vapor is different.

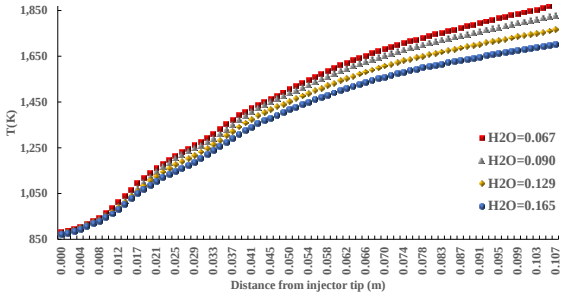

Figure 20: Water vapor effect on temperature variation along axis of symmetry

The results show that increasing the temperature accompanied with increasing water vapor formation affects temperature variation. Maximum difference between cases is about 9.2 percent which occurs in maximum temperature, note that this difference is obtained when water vapor concentration will become about 146% more.

Figure 21 shows Temperature variation in radial axis for 4 cases. The results show that increasing the temperature accompanied with increasing water vapor formation affects temperature variation. Maximum difference between cases is about 9.48 percent which occurs in maximum temperature.

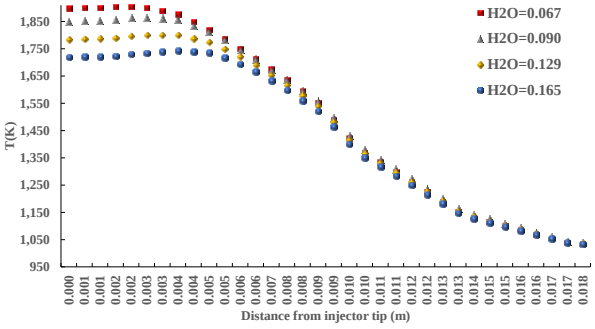

Figure 21. Water vapor effect on radial temperature distribution

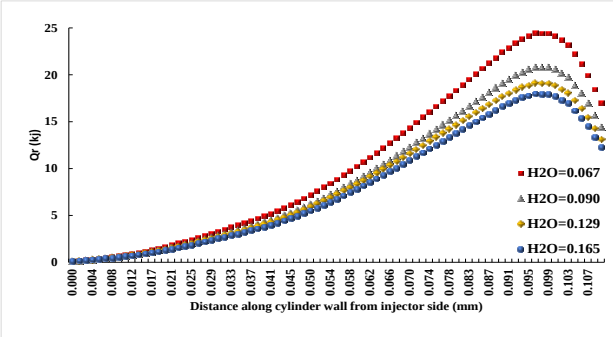

Figure 22: Water vapor effect on heat transfer to wall

Figure 22 shows heat transfer to walls in different water vapor concentration. Results shows that increment of water vapor will decrease the amount of heat received by cylinder wall. Maximum difference is calculated about 28% in case4.

7. Conclusion

In this study, the aim was to find a way to solve combustion and radiation problems, simultaneously, in order to determine radiation effects on temperature distribution and heat transfer to wall of a diesel engine. Results of this study will create a frame work for modeling internal combustion engines heat transfer, considering all modes of heat transfer, especially radiation. in order to model the problem, an open source software OPENFOAM and a solver named soraDieselFOam was used which could model fluid flow using basic fluid mechanics equations (basic mass, momentum and enthalpy equations, species mass conservation and radiation transport), turbulence using RANS model, multi-step chemical reactions, soot formation using Fusco based soot model, conduction and convection heat transfer as suitable terms in basic equation problem, radiation heat transfer using discrete ordinate method(DOM), combustion using Pasr model and Model none gray using wide band model. In the next step, the solver was verified using experimental data of a special burner Mckenna burner. In this study three simplifying assumption are made, first assuming a simple cylinder as model for combustion chamber geometry, second assuming the flow to be axis symmetric and finally ignoring moving walls effect. results shows temperature increases along axis of symmetry. Considering radiation the temperature is calculated less than no radiation case. In distances near injector tip the difference between the two casesis less than 4 percent, and difference between the no radiation and gray case is less than 2 percent, increasing the distance and temperature makes radiation effects more acute and the difference will became more than 11 percent in none gray case and more than 4 percent in gray case. The average temperature difference with no radiation condition is 3.28% in gray and 9% in none gray condition. moreover, there is a difference between calculated temperature in gray and none gray cases, this difference differs between 2.52% to 9% the average temperature difference is 5.92%.

In radial axis as the distance from axis of symmetry increases, the temperature decreases. Considering radiation, the temperature is calculated less than no radiation condition. In

[DOI: 10.22068/ijae.9.1.2919]

distances far from axis of symmetry the difference between the two conditions is less than 5 percent, in distances near the axis, increasing temperature makes radiation effects more acute and the difference will became more than 32 percent. Also there is a difference between calculated temperature in gray and none gray, this difference differs between 2.52% to 9% the average temperature difference is 5.92%.

Result shows that heat transfer to wall is function of temperature and participating media concentration and considering gray media effect can change the result 6.23% to 11.86% and the average difference between gray and none gray radiative heat transfer is 10.07%.

In the next step, effect of soot formation was studied, results shows that increasing the temperature accompanied with increasing soot formation affects temperature variation. Maximum difference between cases is about 7 percent which occurs in maximum temperature. Also increment of soot will decrease the amount of irradiation received by element through the axis of symmetry. The results in the radial axis also shows that increasing the temperature accompanied with increasing soot formation affects temperature variation. Maximum difference between cases is about 6 percent which occurs in maximum temperature and increment of soot will decrease the amount of irradiation received by element through the axis of symmetry. Also Temperature study shows that increasing the temperature accompanied with increasing soot formation affects temperature variation. Maximum difference between cases is about 6 percent which occurs in maximum temperature.

Results of heat transfer to wall study shows that increment of soot will decrease the amount of heat received by cylinder wall. Maximum difference is calculated about 22%.

The last part in this study is to determine the effects of Carbone dioxide and water vapor concentration (two main participating media) on temperature distribution and heat transfer to wall, results show that increasing the temperature accompanied with increasing Carbone Dioxide formation affects temperature variation. Maximum difference between studied cases is about 4.3 percent which occurs in maximum temperature.. Also increment of Carbone dioxide will decrease the amount of heat received by cylinder wall. Maximum difference is calculated about 21% in the cases.

The results of studying water vapor effects shows that increasing the temperature accompanied with increasing water vapor formation affects temperature variation. Maximum difference between cases is about 9.2 percent which occurs in maximum temperature. The results shows that increasing the temperature accompanied with increasing water vapor formation affects temperature variation. Maximum difference between cases is about 9.48 percent which occurs in maximum temperature

Finally the results shows complete compatibility with the theory. Radiation will become more important as the temperature and amount of participating media formation increases, moreover considering the radiation the temperature is calculated less than ignoring radiation. And none gray media considerations are important and can affect the results.

[DOI: 10.22068/ijae.9.1.2919]

References

[1] M. Pishgooie, *A study on the effet of radiation heat transfer on the performance of an internal combustion engines*, PhD Thesis, faculty of mechanical engineering, Department of engineering and technical, shahid bahonar university, kerman, 2017. (in persian)

[2] R. Viskanta, M. P. Mengo, Radiation heat transfer in combustion systems, *Progrss inEnergy and Combustion Science*, Vol. 13, No. 1 , pp. 97-160, 1987.

[3] S. Haider, K. Pang, A.Ivarsson, J. Schramm, Combustion and radiation modeling of laminar premixed flames using OpenFOAM: A numerical investigation of radiative heat transfer in the RADIADE project, *Proceedings ofCongrès International des Moteurs A Combustion Interne Congress(CIMAC)*, Shanghai, China, May 13-16, Paper No. 274, 2013.

[4] M. F. Modest , D. C. Hworth, *Radiative Heat Transfer in Turbulent combustion systems Theory and Applications*, First edition, pp. 1-146, New York: Springer, 2016.

[5] J. B. Heywood, *Internal combustion engines fundementals*, First edition, pp. 668-722, New York: McGraw-Hill, 1988.

[6] G. Woschni, A universally applicable equation for the instantaneous heat transfer coefficient in the internal combustion engine, *Society of Automotive Engineering (SAE) Technical Paper*, paper No. 670931, Vol. 1, No. 1, pp. 3065-3084, 1967.

[7] W. J. D. Annand, Geometry of spherical flame propagation in a disc-shaped combustion chamber, *Journal of mechanical engineering science*, Vol. 12, No. 2, pp. 146-149, 1970.

[8] S. H. Mansouri, J. B. Heywood, K. Radhakrishnan, Divided-Chamber Diesel Engine, Part I: A Cycle-Simulation which predicts performance and emissions, *Society of Automotive Engineering (SAE) Technical Paper*, paper NO. 820273, Vol. 1, No. 1, pp. 89-121, 1982.

[9] S. L.Chang, K. Rhee, Computation of radiation heat transfer in diesel combustion, *Society of Automotive Engineering (SAE) Technical Paper*, paper No. 831332, Vol. 1, No. 1, pp. 130-148, 1983.

[10] C. Blunsdon, W. Malalasekera, J. Dent, Application of the discrete transfer model of thermal radiation in a CFD simulation of diesel engine combustion and heat transfer, *Proceedings of the International fuel and lubrication Meeting*, san Francissco, California, october 19-22, 1992.

[11] Blunsdon, C., Dent, J., and Malalasekera, W., Modelling Infrared Radiation from the Combustion Products in a Spark Ignition Engine, Proceedings on the International fuel and lubrication Meeting, Philadelphia,Pennsylvania, october 18-21, 1993.

[12] S. H. Mansouri, Y. Bakhshan, Studies of NOx, CO, soot formation and oxidation from a direct injection stratified-charge engine using the k–ε turbulence model, *SAGE journal of Meterial science and engineering*, Vol. 215, No. 1, pp. 95-104, 2001.

[13] Y. Bakhshan, G. A. Karim, S. H. Mansouri, study of instantaneous unsteady heat transfer in a rapid Compression-Expansion Machine using k-ε Trbulance model, *Iranian journal of science & Technology*, Transaction B, Vol. 27, No. B3, pp. 607-616, 2001.

[14] H. J. Park, *Development of an in cylinder heat transfer model with variable density effects on thermal boundary layers*, PhD Thesis, university of the Michigan, Michigan, 2009.

[DOI: 10.22068/ijae.9.1.2919]

[15] M. Bovo, *Principles of heat transfer in Internal combustion engines from a modeling standpoint*, PhD Thesis, chalmers university of technology, sweden, 2014.

[16] T. Senčić, V. Medica, O. Bukovac, Soot model validation and development, elsevier advanced engineering journal, Vol. 4, No. 1, pp .75-86, 2010.

[17] T. J. Poinsot, D. Veynante, *Theoretical and Numerical Combustion*, second edition, pp. 25-210, Edwards ,2005

[18] M. Hallaji, K. Mazaheri, Numerical simulation of turbulent non-premixed combustion in diluted hot coflow using PaSR combustion model, Proceedings of MCS congress Chia Laguna Cagliari Sardinia, Italy, September 11-15, 2011

[19] A. Bhave, M. Kraft, Partially stirred reactor model: Analytically solutions and numerical convergence study of PDF/Monte Carlo method, Society for Industrial and Applied Mathematics (SIAM), Vol 25, no 5, pp. 1798-1823, 2004

[20] A. Fusco, A. L. Knox-Kelecy, D. E. Foster, Application of a phenomenological soot model to diesel engine combustion, Proceedings of the International Symposium COMMODIA 94, Yokohama, Japan, July 11-14, 1994

[21] M. F. Modest, Radiative heat transfer, second edition, pp. 263-728, San Diego, San Diego Academic Press, 2003.

[22] S. Haidar, A. Ivarsson, K. M. Pang, S. H. Mansouri, CFD modeling of radiative heat transfer of an in-house helium stabilized laminar premixed flat flame , Proceedings of12th international conference on heat transfer, Fluid mechanics and thermodynamics, July 11-13, Malaga, Spain, 2016

[23] S.S. Penner, Quantitative Molecular Spectroscopy and Gasissivities, First edition, Addison-Wesley, 1959.

[24] M. F. Modest, Radiative heat transfer, second edition, pp. 263-728, San Diego, San Diego Academic Press, 2003.

[25] Y. Liu ,X. Zhang, Analysis of Gas Radiative Transfer Using Box Model and Its Comparison with Gray Band Approximation, Journal of Thermal Science. Vol.12, no. 1, pp.82-88, 2003.

[26] R. Siegel, J. R. Howell, Thermal Radiation Heat Transfer, Forth edition, pp. 419-557, Washington D. C: Hemisphere Publishing Corporation, 1992.

[27] J.F. Widmann, Evaluation of the planck mean absorption coefficients for radiation transport through smoke, journal of Combustion Science and Technology, Vol. 175, no.12,pp. 2299-2308, 2003.

[28] T.K. Bose, High temperature gas dynamics: An Introduction for Physicists and Engineers, Springer, 2005.

[29] Stephen R. Turns, An introduction to combustion: concepts and applications,McGraw-Hill series in mechanical engineering, 1996

[30] G. Pal, M.F. Modest, k-distribution methods for radiation calculations in high pressure combustion,Journal of Thermo physics and Heat Transfer, Vol.27, No.3, pp. 584-587,2013

[DOI: 10.22068/ijae.9.1.2919]